Activation of inflammasomes in podocyte injury of mice on the high fat diet: Effects of ASC gene deletion and silencing

Krishna M. Boini [a,*], Min Xia [a], Justin M. Abais [a], Guangbi Li [a], Ashley L. Pitzer [a], Todd W.B. Gehr [b], Yang Zhang [a], Pin-Lan Li [a,**]

[a] Department of Pharmacology and Toxicology, Virginia Commonwealth University, School of Medicine, Richmond, VA 23298, USA
[b] Department of Internal Medicine, Virginia Commonwealth University, School of Medicine, Richmond, VA 23298, USA

ARTICLE INFO

ABSTRACT

Inflammasome, an intracellular inflammatory machinery, has been reported to be involved in a variety of chronic degenerative diseases such as atherosclerosis, autoinflammatory diseases and Alzheimer's disease. The present study hypothesized that the formation and activation of inflammasomes associated with apoptosis associated speck-like protein (ASC) are an important initiating mechanism resulting in obesity-associated podocyte injury and consequent glomerular sclerosis. To test this hypothesis, Asc gene knockout ($Asc^{-/-}$), wild type ($Asc^{+/+}$) and intrarenal Asc shRNA-transfected wild type (Asc shRNA) mice were fed a high fat diet (HFD) or normal diet (ND) for 12 weeks to produce obesity and associated glomerular injury. Western blot and RT-PCR analyses demonstrated that renal tissue Asc expression was lacking in $Asc^{-/-}$ mice or substantially reduced in Asc shRNA transfected mice compared to $Asc^{+/+}$ mice. Confocal microscopic and co-immunoprecipitation analysis showed that the HFD enhanced the formation of inflammasome associated with Asc in podocytes as shown by colocalization of Asc with Nod-like receptor protein 3 (Nalp3). This inflammasome complex aggregation was not observed in $Asc^{-/-}$ and local Asc shRNA-transfected mice. The caspase-1 activity, IL-1β production and glomerular damage index (GDI) were also significantly attenuated in $Asc^{-/-}$ and Asc shRNA-transfected mice fed the HFD. This decreased GDI in $Asc^{-/-}$ and Asc shRNA transfected mice on the HFD was accompanied by attenuated proteinuria, albuminuria, foot process effacement of podocytes and loss of podocyte slit diaphragm molecules. In conclusion, activation and formation of inflammasomes in podocytes are importantly implicated in the development of obesity-associated glomerular injury.

© 2014 Elsevier B.V. All rights reserved.

1. Introduction

Obesity has greatly increased in Western countries over the last three decades [1–5]. The prevalence of obesity (body mass index BMI 30 kg/m^2) is 66% in the United States and between 7 and 37% in Europe [1–5]. Obesity is associated with and contributes to the development of type 2 diabetes mellitus, cardiovascular diseases, and non-diabetic chronic kidney disease (CKD) [6]. CKD is now considered as one of the strongest risk factors for the morbidity and mortality in obese patients [7,8]. Experimental and clinical studies reveal that adipose tissue, especially visceral fat generates bioactive substances that contribute to the pathophysiologic renal hemodynamic and structural changes leading to obesity-associated glomerular injury [9]. So far a few mechanisms have been proposed for the obesity-induced CKD including chronic inflammation, abnormal vascular remodeling, rise in renal plasma flow, hyperfiltration and renal lipotoxicity [10]. However, the underlying molecular mechanisms involved in obesity-induced glomerular injury, specifically, the early initiating processes responsible for the glomerular injury during obesity, remain poorly understood.

In this regard, the inflammasome is a newly identified cellular machinery responsible for the activation of innate inflammatory processes [11] and instigation of inflammatory responses during a variety of chronic degenerative diseases such as atherosclerosis [12,13] and Alzheimer's disease [14,15] as well as various auto inflammatory diseases including obesity, diabetes, gout, silicosis, and acetaminophen-induced liver toxicity [16–22]. Among different kinds of inflammasomes, the NALP3 inflammasome is the most fully characterized in a variety of mammalian cells. NALP3 inflammasome is a proteolytic complex composed of the Nod-like receptor protein 3 (NALP3), the adaptor protein apoptosis associated speck-like protein (Asc), and caspase-1 [22], which is vital for the production of mature IL-1β in response to a variety of agonists or stimuli. It has been reported that IL-1β is an important cytokine with a broad range of biological activities [19,23] involved in kidney injury and repair [24–26] and that in glomeruli it is mainly produced by podocytes [27,28]. The active mature interleukin-1β (IL-1β)

* Correspondence to: K.M. Boini, Department of Pharmacology and Toxicology, Virginia Commonwealth University, School of Medicine, 410 N, 12th Street, Richmond, VA 23298, USA. Tel.: +1 804 828 4769; fax: +1 804 828 4794.
** Correspondence to: P.L. Li, Department of Pharmacology and Toxicology, Virginia Commonwealth University, School of Medicine, 410 N, 12th Street, Richmond, VA 23298, USA. Tel.: +1 804 828 4769; fax: +1 804 828 4793.
E-mail addresses: kmboini@vcu.edu (K.M. Boini), pli@vcu.edu (P.-L. Li).

is formed by cleaving inactive pro IL-1β precursor via caspase-1, which is activated in a large multiprotein complex, namely, the inflammasome [23,29–35]. The Nalp3 inflammasome has been reported to be activated by several stimulants such as ATP, monosodium urate crystals (MSU) [20] or β-amyloid [36]. It has been shown that in the kidney NALP3 inflammasomes are one of the triggering mechanisms responsible for hyperhomocysteinemia-induced glomerular injury, furthermore it participates in acute ischemia/reperfusion-induced kidney injury, unilateral ureteral obstruction-induced renal damage and non-diabetic human kidney disease [25,26,37–40]. However, it remains unknown whether obesity activates the NALP3 inflammasomes and thereby results in glomerular injury in the kidney.

The present study hypothesized that the formation and activation of NALP3 inflammasomes are an important initiating mechanism resulting in obesity-associated glomerular injury. To test our hypothesis, we used Asc$^{-/-}$ and local Asc gene silencing strategies to examine the role of inflammasomes-associated with Asc in obesity-induced glomerular injury. Because ASC is a key inflammasome adaptor for NALP3 inflammasomes [20,41], gene knockout or locally silencing the Asc gene may mainly block the formation and activation of NALP3 inflammasomes in podocytes. Our results demonstrate that the formation and activation of NALP3 inflammasomes in podocytes may be importantly implicated in the development of glomerular injury and ultimate sclerosis during obesity.

2. Materials and methods

2.1. Animals

Eight weeks old male Asc$^{-/-}$ mice and their wild type littermates were used in the present study [11,41]. The mice were fed either a low fat diet (LFD: D 12450B, 10 kcal % fat, Research Diets, New Brunswick, NJ) or a high fat diet (HFD: D 12492, 60 kcal % fat, Research Diets, New Brunswick, NJ) for 12 weeks [42–44]. In another series, eight week old male C57BL/6J or DBA/2J wild type mice (Jackson Laboratories, Bar Harbor, ME), Asc shRNA or a scrambled shRNA (Origene, Rockville, MD, USA) plasmid with a luciferase expression vector was co-transfected into the kidneys via intrarenal artery injection using the ultrasound microbubble system as we described previously [45]. After the delivery of plasmids into the kidney, mice were fed either a normal diet or HFD for 12 weeks. All protocols were approved by the Institutional Animal Care and Use Committee of the Virginia Commonwealth University.

2.2. Caspase-1 activity, IL-1β production, plasma insulin, triglycerides and total cholesterol

Caspase-1 activity in glomeruli was measured by a commercially available colorimetric assay kit (Biovision, Mountain View, CA). IL-1β production in glomeruli was measured by a commercially available ELISA kit (R&D System, Minneapolis, MN), according to the manufacturer's instructions [26,46]. Plasma concentrations of insulin were determined using an ELISA kit (Crystal Chem, USA). Total cholesterol (Cayman Chemical Company, USA) and triglycerides (Sigma) were analyzed using a colorimetric assay.

2.3. Morphological examinations

The fixed kidneys were paraffin-embedded, and sections were prepared and stained with Periodic acid–Schiff stain. Glomerular damage index (GDI) was calculated from 0 to 4 on the basis of the degree of glomerulosclerosis and mesangial matrix expansion as described previously [47,48]. In general, we counted 50 glomeruli in total in each kidney slice under microscope, when each glomerulus was graded level 0–4 damages. 0 represents no lesion, 1 + represents sclerosis of <25% of the glomerulus, while 2 +, 3 +, and 4 + represent sclerosis of 25% to 50%, >50% to 75%, and >75% of the glomerulus. A whole kidney average sclerosis index was obtained by averaging scores from counted glomeruli. This observation was examined by two independent investigators who were blinded to the treatment of the experimental groups [26,45–48].

2.4. Urinary total protein and albumin excretion measurements

The 24-hour urine samples were collected using metabolic cages and subjected to total protein and albumin excretion measurements, respectively [45,47,48]. Total protein content in the urine was detected by Bradford method using a UV spectrophotometer. Urine albumin was detected using a commercially available albumin ELISA kit (Bethyl Laboratories, Montgomery, TX).

2.5. Delivery of Asc shRNA into the kidneys by ultrasound-microbubble technique

Asc shRNA or a scrambled shRNA plasmid with a luciferase expression vector was used to co-transfect the kidneys via intrarenal artery injection using the ultrasound-microbubble system. These experiments were performed to test whether local silencing Asc gene expression in podocytes alters obesity-induced glomerular injury. A full description of the procedures for the ultrasound-microbubble gene transfer technique can be found in our previous studies [26,45,47]. To monitor the efficiency of gene expression through somatic plasmid transfection daily, mice were anesthetized with isoflurane, and an aqueous solution of luciferin (150 mg/kg) was injected intraperitoneally 5 min before imaging. The anesthetized mice were imaged using the IVIS200 in vivo molecular imaging system (Xenogen, Hopkinton, MA, USA). Photons emitted from luciferase-expressing cells within the animal body and transmitted through tissue layers were quantified over a defined period of time ranging up to 5 min using the software program Living Image as program (Xenogen). The inhibitory efficiency of gene expression by Asc shRNA was further confirmed by the detection of Asc level in mouse renal cortex using real-time RT-PCR.

2.6. Real-time reverse transcription polymerase chain reaction (RT-PCR)

Total RNA from isolated mouse renal tissue was extracted using TRIzol reagent (Invitrogen, Carlsbad, CA) according to the protocol as described by the manufacturer. RNA samples were quantified by measurement of optic absorbance at 260 nm and 280 nm in a spectrophotometer. The concentrations of RNA were calculated according to A260. Aliquots of total RNA (1 μg) from each sample were reverse-transcribed into cDNA according to the instructions of the first strand cDNA synthesis kit manufacturer (Bio-Rad, Hercules, CA). Equal amounts of the reverse transcriptional products were subjected to PCR amplification using SYBR Green as the fluorescence indicator on a Bio-Rad iCycler system (Bio-Rad, Hercules, CA) [26,45,47]. The primers used in this study were synthesized by Operon (Huntsville, AL, USA) and the sequences were: for Asc sense ACAGAAGTGGACGGAGTGCT, antisense CTCCAGGTCCATCACCAAGT; for Podocin sense GTGGAAGCTGAGGCACAAAGAC, antisense CAGCGACTGAAGA GTGTGCAAG; for desmin sense CAGTCCTACACCTGCGAGATT, antisense GGCCA TCTTCACATTGA GC; for MCP-1 sense ACCACAGTCCATGCCATCAC, antisense TTGAGGTG GTTGTGGAAAAG; for IL-18 sense GCTTGAATCTAAATTATCAGTC, antisense GAAGATTCAAATTGCATCTTAT and for β-actin sense TCGCTGCG CTGGTCGTC, antisense GGCCTCGTCACCCACATAGGA.

2.7. Confocal microscopic detection of inflammasome protein complexes

Indirect immunofluorescent staining was used to determine colocalization of the inflammasome proteins in glomeruli of the mouse kidney, which indicate the formation of inflammasome molecular complex. Frozen kidney tissue slides were fixed in acetone and then incubated

overnight at 4 °C with either goat anti-Nalp3 (1:200) and rabbit anti-Asc (1:50), or goat anti-Nalp3 (1:200) and mouse anti-caspase-1 (1:100). To further confirm the presence of the inflammasomes specifically in podocytes of the mouse glomeruli, Nalp3 or caspase-1 was co-incubated with a podocin antibody (1:400; Sigma, St. Louis, MO). Double immunofluorescent staining was achieved by incubating with either Alexa-488 or Alexa-555-labeled secondary antibodies for 1 h at room temperature. After washing, slides were mounted with a DAPI-containing mounting solution, and then observed with a confocal laser scanning microscope (Fluoview FV1000, Olympus, Japan). As previously described [26,47], images were analyzed by the Image Pro Plus 6.0 software (Media Cybernetics, Bethesda, MD), where colocalization was measured and expressed as the Pearson Correlation Coefficient (PCC).

2.8. Transmission electron microscopy (TEM)

For TEM observation of ultrastructural changes in podocytes, the mouse kidneys were perfused with a fixative containing 3% glutaraldehyde and 4% paraformaldehyde in 0.1 M phosphate buffer. After fixation and dehydration with ethanol, the samples were embedded in Durcupan resin for ultra-thin sectioning and TEM examination by the VCU electron microscopy core facility [26,49].

2.9. Immunohistochemistry

Kidneys were embedded with paraffin and 5 mm sections were cut from the embedded blocks. After heat-induced antigen retrieval, CD43 staining of T cells [46,50] required citrate buffer antigen retrieval. After a 20 min wash with 3% H_2O_2 and 30 min blocking with serum, slides were incubated with primary antibodies diluted in phosphate-buffered saline (PBS) with 4% serum. Anti-CD43 (1:50; Santa Cruz Biotechnology, Santa Cruz, CA) antibody was used in this study. After incubation with primary antibody overnight, the sections were washed in PBS and incubated with biotinylated IgG (1:200) for 1 h and then with streptavidin-HRP for 30 min at room temperature. 50 μl of DAB was added to each kidney section and stained for 1 min. After washing, the slides were counterstained with hematoxylin for 5 min. The slides were then mounted and observed under a microscope in which photos were taken.

2.10. Statistical analysis

Data are provided as arithmetic means ± SEM; n represents the number of independent experiments. All data were tested for significance using ANOVA or paired and unpaired Student's t-tests as applicable. The glomerular damage index was analyzed using a nonparametric Mann–Whitney rank sum test. Only results with $P < 0.05$ were considered statistically significant.

3. Results

3.1. Characterization of Asc gene knockout mice

As shown in Fig. 1A, Asc knockout ($Asc^{-/-}$) and wild type ($Asc^{+/+}$) were genotyped using PCR. Detection of a PCR product at 260 indicates $Asc^{-/-}$, while a PCR product of 450 bp indicates $Asc^{+/+}$ mice. Western blot analysis revealed that Asc protein was hardly detected in the glomeruli of $Asc^{-/-}$ mice, but it was enriched in the glomeruli of $Asc^{+/+}$ mice (Fig. 1B). Furthermore, real time RT-PCR analysis also showed that Asc mRNA expression was not detectable in the glomeruli of $Asc^{-/-}$ mice (Fig. 1C), confirming the Asc gene deletion in mice. The body weight was similar in $Asc^{+/+}$ and $Asc^{-/-}$ mice fed a normal diet. The high fat diet (HFD) significantly increased the body weight in $Asc^{+/+}$ mice compared to normal diet-fed mice. However, $Asc^{-/-}$ mice attenuated HFD-induced increase in body weight ($Asc^{+/+}$ mice: 44.6 ± 2.0 vs. 26.2 ± 1.41 g of control and $Asc^{-/-}$ mice: 33.4 ± 8.6 vs.
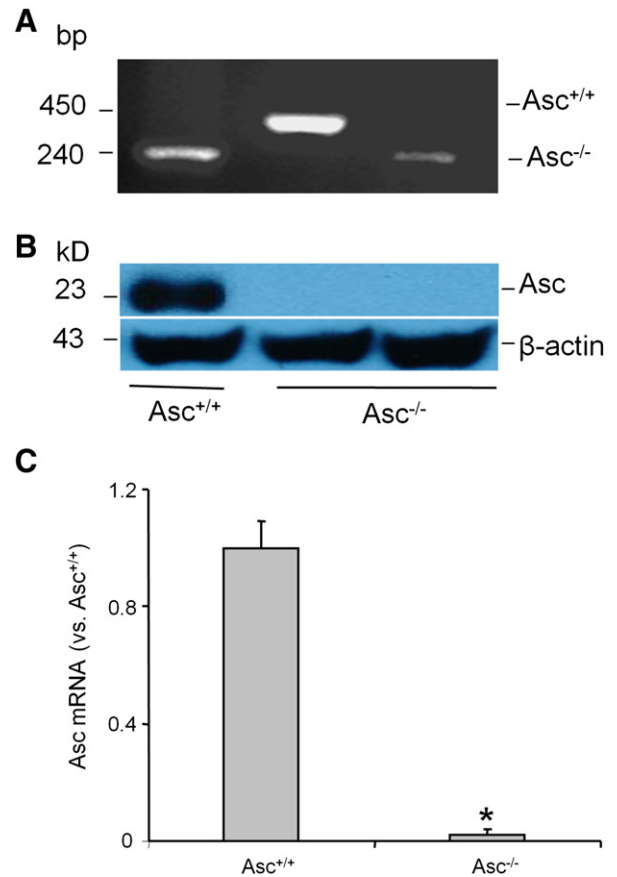

Fig. 1. Genotyping and Asc expression in $Asc^{+/+}$ and $Asc^{-/-}$ mice. A. Genotyping in $Asc^{+/+}$ and $Asc^{-/-}$ mice. Detection of PCR product at 450 bp represents $Asc^{+/+}$ mice, while a PCR product of 260 bp represents $Asc^{-/-}$ mice. B. Western blot analysis of Asc protein expression in mice. C. Values are arithmetic means ± SD (n = 4 each group) of Asc mRNA expression in $Asc^{+/+}$ and $Asc^{-/-}$ mice. *Significant difference ($P < 0.05$) compared to the values from $Asc^{+/+}$ mice.

26.0 ± 0.8 g of control at week 10). HFD significantly increased the plasma glucose, insulin, total cholesterol and triglyceride levels in $Asc^{+/+}$ compared to control mice. However, $Asc^{-/-}$ mice significantly attenuated the HFD-induced blood glucose, plasma insulin concentrations but did not alter the plasma total cholesterol and triglyceride levels (Table 1). These data demonstrate that obesity was induced in HFD-fed mice.

3.2. Formation and activation of podocyte Nalp3 inflammasomes in obesity

As shown in Fig. 2A, confocal microscopic analysis demonstrated that HFD increased the colocalization of Nalp3 with Asc (yellow spots) or Nalp3 with caspase-1 (yellow spots) in glomeruli of $Asc^{+/+}$ mice compared to normal diet (ND)-fed mice. Furthermore, colocalization of Nalp3 with podocin (podocyte marker) indicates enrichment of Nalp3 in podocytes (yellow spots). However, in $Asc^{-/-}$ mice such

Table 1
Blood glucose, plasma insulin, triglycerides, total cholesterol concentrations in $Asc^{+/+}$ and $Asc^{-/-}$ mice fed a ND or high fat diet treatment.

Parameters	$Asc^{+/+}$ ND	$Asc^{-/-}$ ND	$Asc^{+/+}$ HFD	$Asc^{-/-}$ HFD
Blood glucose (mg/dl)	121 ± 2.0	111 ± 10.3	156 ± 9.0*	110.9 ± 23.0#
Plasma insulin (ng/ml)	0.9 ± 0.1	0.8 ± 0.2	3.6 ± 0.4*	1.5 ± 0.4#
Triglycerides (mg/dl)	64 ± 4.6	59 ± 7.0	113 ± 13*	83 ± 7
Total cholesterol (mg/dl)	149 ± 4.3	145 ± 8.0	178 ± 8*	162 ± 8

ND: Normal diet, HFD: high fat diet. N = 5–6 in each group. The data was expressed as mean ± SEM.
* $P < 0.05$ as compared with $Asc^{+/+}$ ND. # Significant difference ($P < 0.05$) compared to the values from $Asc^{+/+}$ mice receiving the HFD.
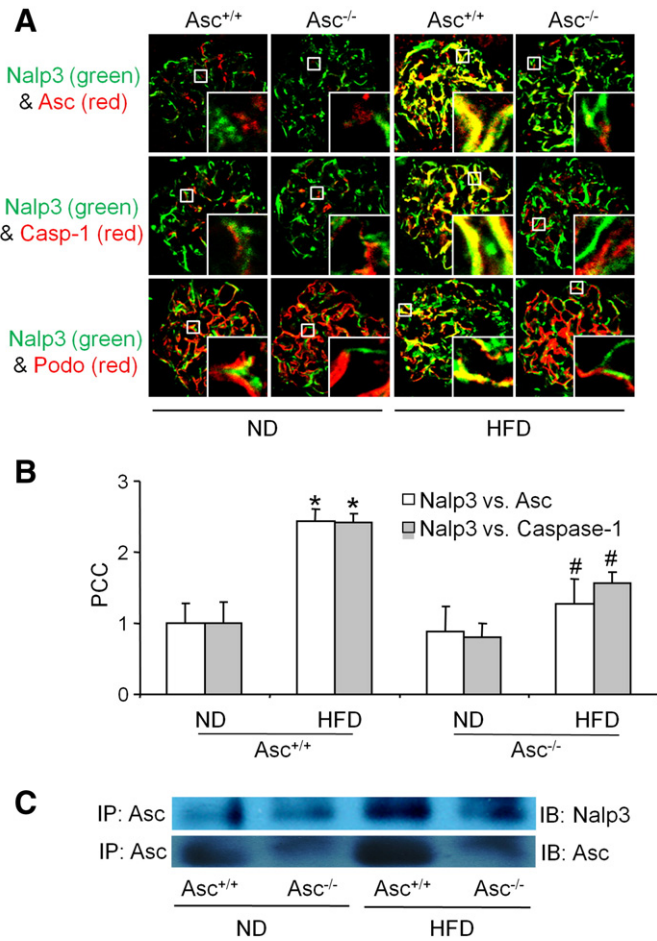
Fig. 2. Formation of podocyte Nalp3 inflammasomes in glomeruli of $Asc^{+/+}$ and $Asc^{-/-}$ mice fed with ND or high fat diet. A. Overlaid images (yellow spots) show the colocalization of Nalp3 (green) with Asc (red), Nalp3 (green) with caspase-1 (red) and Nalp3 (green) with podocin (red) in mouse glomeruli. B. Summarized data shows the fold changes of Pearson coefficient correlation (PCC) for the colocalization of Nalp3 with Asc and Nalp3 with caspase-1 in glomeruli of $Asc^{+/+}$ and $Asc^{-/-}$ mice fed with either ND or HFD. C. Immunoprecipitation and Western blot analysis of the interaction of Nalp3 with ASC in glomeruli of either ND or HFD fed mice. Casp-1: Caspase-1 and Podo: Podocin. *Significant difference ($P < 0.05$) compared to the values from ND fed mice, #significant difference ($P < 0.05$) compared to the values from $Asc^{+/+}$ mice receiving the HFD.

colocalizations were not detected (Fig. 2A). These results suggest the formation of Nalp3 inflammasomes in glomeruli of obese mice. The summarized data of quantitative colocalization of Nalp3 with Asc or caspase-1 in glomeruli of mice were shown in Fig. 2B. In addition, coimmunoprecipitation (Co-IP) experiments also demonstrated that the HFD significantly increased the binding of Asc together with Nalp3 in glomeruli of $Asc^{+/+}$ mice compared to ND, which was again attenuated in $Asc^{-/-}$ mice fed a HFD (Fig. 2C). These results further confirm the formation of Nalp3 inflammasomes in glomeruli of obese mice, which is associated with a normal expression of Asc gene. Biochemical analysis showed that the HFD significantly increased caspase-1 activity and IL-1β production in glomeruli of $Asc^{+/+}$ mice but not in $Asc^{-/-}$ mice (Fig. 3). In addition, $Asc^{-/-}$ mice significantly attenuated the HFD-induced MCP-1 and IL-18 expression compared to $Asc^{+/+}$ mice (Table 2), suggesting an abolishment of activation of podocyte Nalp3 inflammasomes during obesity by deletion of mouse Asc gene.

3.3. Contribution of Nalp3 inflammasomes to obesity-induced glomerular inflammation and injury

We also detected the inflammatory response in glomeruli using Immunohistochemical assay with antibodies against surface antigen of
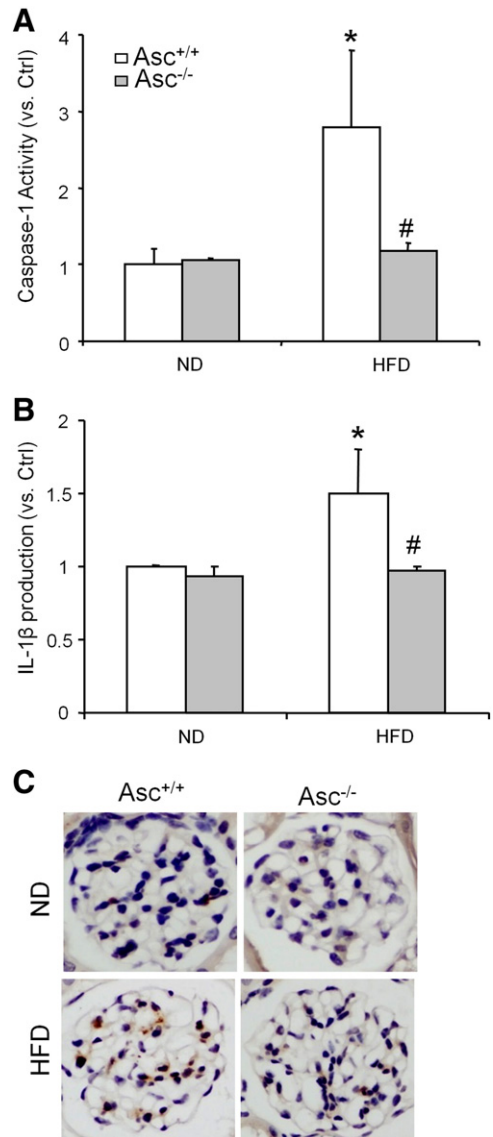

Fig. 3. Activation of podocyte Nalp3 inflammasomes in glomeruli of $Asc^{+/+}$ and $Asc^{-/-}$ mice fed with ND or high fat diet. Values are arithmetic means ± SD (n = 6 each group) of caspase-1 activity (A), cleaved IL-1β concentration (B), IL-1B production (C) in glomeruli of $Asc^{+/+}$ and $Asc^{-/-}$ mice fed with either ND or HFD. *Significant difference ($P < 0.05$) compared to the values from ND fed mice, #significant difference ($P < 0.05$) compared to the values from $Asc^{+/+}$ mice receiving the HFD.

mouse T-cell (anti-CD43). It was found that the HFD-induced T-cell infiltration (CD43 + staining) or aggregation within the glomeruli of obese $Asc^{+/+}$ mice. However, the HFD fed $Asc^{-/-}$ glomeruli had relatively less T-cell infiltration compared to the HFD-fed $Asc^{+/+}$ mice (Fig. 4A). These results support the view that obesity leads to glomerular

Table 2
MCP-1 and IL-18 expression in glomeruli of $Asc^{+/+}$ and $Asc^{-/-}$ mice fed a ND or high fat diet treatment.

Parameters	$Asc^{+/+}$ ND	$Asc^{-/-}$ ND	$Asc^{+/+}$ HFD	$Asc^{-/-}$ HFD
MCP-1	1.0 ± 0.1	0.8 ± 0.1	3.5 ± 0.4*	0.9 ± 0.1#
IL-18	1.0 ± 0.1	0.8 ± 0.1	1.6 ± 0.4*	1.1 ± 0.1#

Quantitative real time PCR analysis was performed and the values were normalized against β-actin. The data was expressed as mean ± SEM. ND: Normal diet, HFD: high fat diet. n = 4 in each group. * Significant difference ($P < 0.05$) compared to the values from control mice on the normal diet, # Significant difference ($P < 0.05$) compared to versus values from mice fed the HFD.

inflammation through Nalp3 inflammasome activation in mice. Further functional studies showed that urinary albumin excretion was significantly higher in HFD-fed mice compared to ND-fed mice. The $Asc^{-/-}$ mice had significantly decreased urinary albumin excretion compared to $Asc^{+/+}$ mice (Fig. 4B). Furthermore, HFD-fed $Asc^{+/+}$ mice produced significant morphological changes in the glomeruli including mesangial expansion, capillary collapse and increased cellularity (Fig. 4C), which was significantly attenuated in the $Asc^{-/-}$ mice. The glomerular damage index (GDI) was significantly higher in $Asc^{+/+}$ mice fed a HFD compared to the ND. However, the HFD-induced increase in GDI was significantly attenuated in $Asc^{-/-}$ mice (Fig. 4D). These results strongly suggest that the formation and activation of inflammasome associated with ASC are an important early mechanism responsible for glomerular inflammation and injury in obese mice.

Further experiments were performed to test whether inflammasome-mediated glomerular injury is due to podocyte dysfunction or injury. Real time RT-PCR analysis showed that podocin expression (podocyte injury marker) was found markedly reduced in glomeruli of HFD-fed $Asc^{+/+}$ mice than in ND-fed mice, indicating podocyte injury. The $Asc^{-/-}$ mice showed significantly less HFD-induced reduction of podocin expression (Fig. 5A). In contrast, another podocyte injury marker, desmin was found markedly increased in glomeruli of $Asc^{+/+}$ mice on the HFD compared to those on the normal diet. However, this increased desmin expression did not occur in $Asc^{-/-}$ mice even on the HFD (Fig. 5B and C). Under transmission electron microscopy (TEM), the intact structure of podocyte foot processes shown in glomeruli of mice were observed in ND-fed mice, while it was destroyed in HFD-fed mice, as shown by evident foot process effacement in HFD-fed $Asc^{+/+}$ mice. In contrast, podocytes of HFD fed $Asc^{-/-}$ had relatively normal ultrastructures (Fig. 5D), indicating attenuated podocyte injury within the glomeruli of obese mice.

3.4. Local silencing of Asc gene attenuated the inflammasome formation in glomeruli of obese mice

To further determine whether local inhibition of Asc gene expression alters the obesity-induced Nalp3 inflammasome activation and formation in podocytes of mice, shRNA strategy was used to silence this gene in the kidney and then observe the changes in body weight, glomerular function and pathology in obese mice. As illustrated in Fig. 6, using IVIS in vivo molecular imaging system, luciferase gene expression co-transfected with Asc shRNA could be detected even on the fourth day after the kidney was transfected by ultrasound-microbubble plasmid introduction. In the hemi-dissected kidney, all of the cortical regions were observed to exhibit efficient gene transfection as shown in green and red fluorescence (Fig. 6A and B). This result is consistent with previous studies showing that ultrasound-microbubble gene introduction is an efficient technique for delivery of the gene into the glomerular cells, vascular endothelial cells, and fibroblasts [42]. Such in vivo monitoring of gene expression was used to guide functional studies. The efficiency of local Asc gene silencing was also examined by measurement of mRNA expression when animals were sacrificed after the completion of functional studies. Real time PCR analysis demonstrated that Asc mRNA expression was significantly decreased in C57BL/6J WT mice transfected with Asc shRNA compared to control mice (scramble shRNA). The HFD significantly increased the Asc mRNA expression in glomeruli from mice receiving scrambled shRNA compared to ND-fed mice, but it had no effect on Asc mRNA abundance in mice receiving Asc shRNA (Fig. 6C). Asc shRNA transfection did not alter the Asc mRNA expression in liver, heart and adipose tissues compared to control (scramble shRNA) mice (Table 3). Furthermore, the Asc shRNA transfection did not alter the body weight in ND and HFD fed mice (scramble shRNA: 40.8 ± 2.5 vs. 26.0 ± 1.2 g of control and Asc
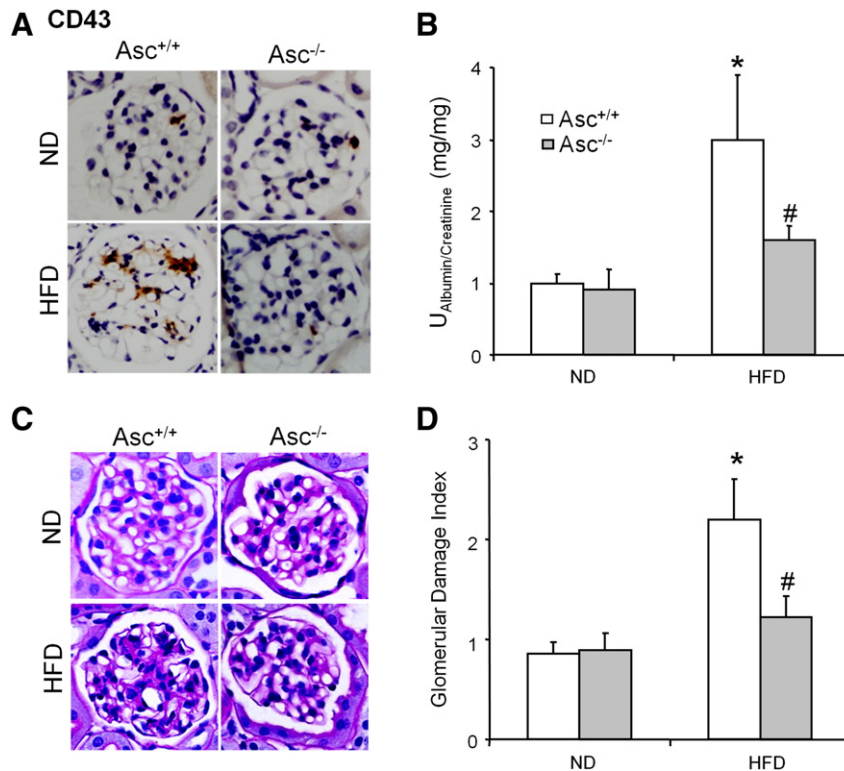

Fig. 4. Effects of the normal diet and HFD on glomerular injury in $Asc^{+/+}$ and $Asc^{-/-}$ mice. A: $Asc^{-/-}$ mice prevented the increased expression and staining of T-cell marker CD43 in glomeruli of $Asc^{+/+}$ on high fat diet. B: Values are arithmetic means $\pm$ SD (n = 6 each group) of urinary albumin excretion in $Asc^{+/+}$ and $Asc^{-/-}$ mice with or without the HFD. C: Photomicrographs show typical glomerular structure (original magnification, ×400) in $Asc^{+/+}$ and $Asc^{-/-}$ mice fed with or without HFD. D: Summarized data of glomerular damage index (GDI) by semi-quantitation of scores in 4 different groups of mice (n = 6 each group). For each kidney section, 50 glomeruli were randomly chosen for the calculation of GDI. *Significant difference ($P < 0.05$) compared to the values from ND fed mice, #significant difference ($P < 0.05$) compared to the values from $Asc^{+/+}$ mice receiving the HFD.
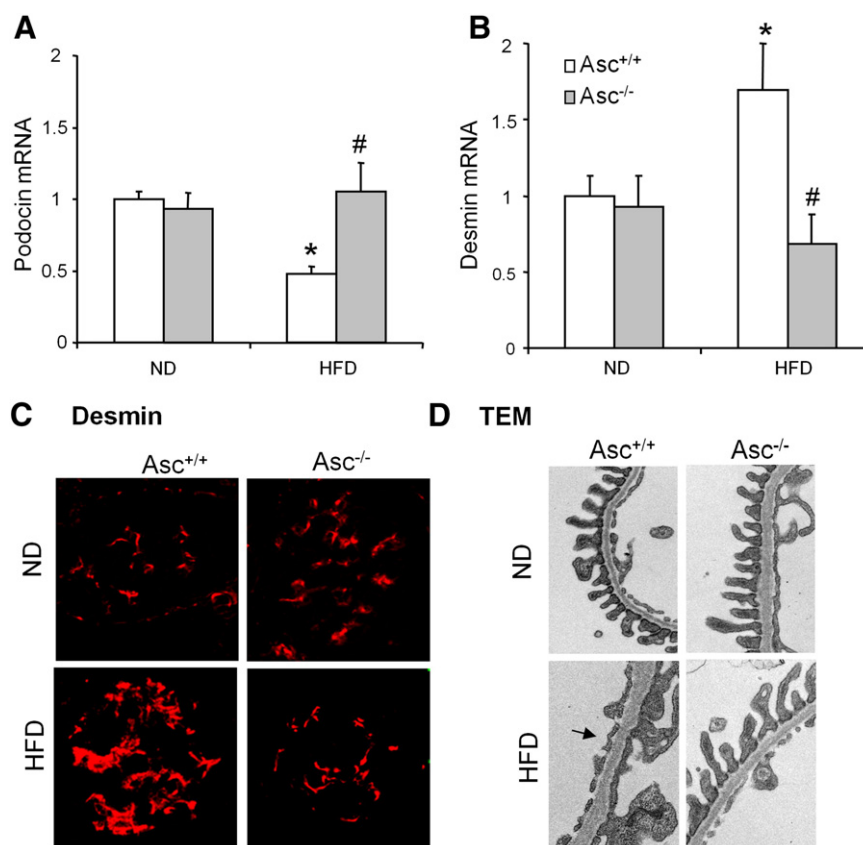
Fig. 5. Immunofluorescence staining and expression of desmin and podocin in glomeruli from $Asc^{-/-}$ and $Asc^{+/+}$ mice fed a ND or HFD. A. Real-time RT-PCR analysis showing changes in the expression of podocin in the glomeruli from different groups of mice (n = 6 per group). B. Real-time RT-PCR analysis showing changes in the expression of desmin in the glomeruli from different groups of mice (n = 6 per group). C. Typical images of desmin staining in glomeruli from $Asc^{-/-}$ and $Asc^{+/+}$ mice with or without HFD. D. $Asc^{-/-}$ improved podocyte ultrastructure in HFD treated mice as shown by TEM examinations. The arrow denotes the area of foot process effacement in $Asc^{+/+}$ mice on the HFD. Images are representative of 5 TEM images per kidney from 2 mice per group. Original magnification: ×8000. *Significant difference ($P < 0.05$) compared to the values from ND fed mice, #Significant difference ($P < 0.05$) compared to the values from $Asc^{+/+}$ mice receiving the HFD.

shRNA mice: 42.4 ± 2.2 vs. 27.3 ± 0.9 g of control at week 10), indicating that local silencing of *Asc* gene prevented the obesity-induced inflammasome activation in glomeruli.

Moreover, we determined whether *Asc* gene silencing locally in the kidney may attenuate the Nalp3 inflammasome formation and protects against the glomerular injury in obese mice. As illustrated in Fig. 7, the HFD increased the colocalization of Nalp3 with Asc and Nalp3 with caspase-1 in glomeruli of mice. However, Asc shRNA transfection significantly attenuated such HFD-induced colocalization of Nalp3 with Asc and Nalp3 with caspase-1 (Fig. 7A and B). Consistent with decreased aggregation of inflammasome components in the glomeruli, HFD-induced caspase-1 activity was also markedly attenuated in Asc shRNA transfected mice (Fig. 7C). Next, we determined whether *Asc* gene silencing locally in the kidney may also protect obesity-induced podocyte injury and consequent glomerular disease. The urinary protein excretion was similar in both scrambled and Asc shRNA transfected mice fed on the ND. HFD treatment significantly increased the urinary total protein excretion when compared to the ND-fed mice. However, Asc shRNA transfection significantly attenuated HFD-induced increases in urinary total protein excretion (Fig. 8A). Furthermore, we found that podocyte marker podocin was markedly reduced in glomeruli of scrambled shRNA transfected mice on the HFD compared to those on the ND. However, this reduced podocin expression or production did not occur in Asc shRNA transfected mouse kidney even on the HFD (Fig. 8B and C). In addition, under TEM the intact structure of podocyte foot processes shown in glomeruli of mice was observed in ND-fed mice, while it was destroyed in HFD-fed mice, as shown by evident foot process effacement in scramble shRNA transfected mice on the HFD. In contrast,

podocytes of HFD fed Asc shRNA transfected mice had relatively normal ultrastructures (Fig. 8D).

Furthermore, we used DBA/2J, another strain of wild type mice to determine whether *Asc* gene silencing locally in the kidney also attenuates the Nalp3 inflammasome formation and protects against the glomerular injury in obese mice. As illustrated in Supplemental Fig. 1, the HFD increased the colocalization of Nalp3 with Asc and Nalp3 with caspase-1 in glomeruli of mice. However, Asc shRNA transfection significantly attenuated such HFD-induced colocalization of Nalp3 with Asc and Nalp3 with caspase-1 (Supplemental Fig. 1A and B). Consistent with decreased aggregation of inflammasome components in the glomeruli, HFD-induced IL-1β production was also markedly attenuated in Asc shRNA transfected mice (Supplemental Fig. 1C). The urinary total protein excretion and glomerular damage index were similar in both scrambled and Asc shRNA transfected mice fed on the ND. HFD treatment significantly increased the urinary total protein excretion when compared to the ND-fed mice. However, Asc shRNA transfection significantly attenuated HFD-induced increases in urinary total protein excretion and glomerular damage index (Supplemental Fig. 2A and B). In addition, we found that podocyte marker podocin was markedly reduced in glomeruli of scrambled shRNA transfected mice on the HFD compared to those on the ND. However, this reduced podocin expression or production did not occur in Asc shRNA transfected mouse kidney even on the HFD (Supplemental Fig. 2C). In contrast, desmin had more profound abundance in glomeruli of HFD fed mice compared with that in ND-fed mice. Asc shRNA transfection abrogated the HFD-induced increase in desmin expression (Supplemental Fig. 2D).
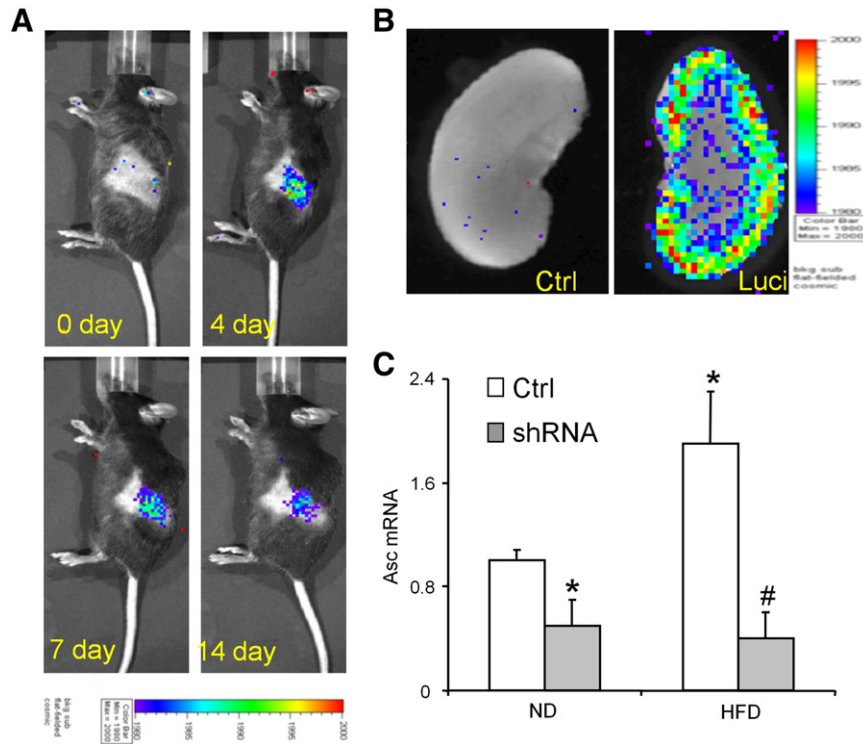
Fig. 6. Renal Asc gene silencing efficiency in C57BL/6J mice with or without the high fat diet. A: Daily imaging confirmation of gene transfection in the kidney by an in vivo molecular imaging system. B: Localization of transfected gene expression in the hemidissected kidney on day 12 after gene delivery. C: Values are arithmetic means ± SD (n = 4–8 each group) of Asc mRNA expression in ND or high fat diet-fed C57BL/6J mice with or without Asc shRNA transfection. *Significant difference ($P < 0.05$) compared to the values from control mice fed on the normal diet, #significant difference ($P < 0.05$) compared to the values from mice on the high fat diet.

4. Discussion

The major goal of the present study is to determine whether inflammasomes are activated in glomerular podocytes and thereby lead to podocyte dysfunction and subsequent glomerular injury during obesity. We demonstrated that HFD-induced increases in NALP3 inflammasome formation and activation in glomeruli, which result in glomerular inflammation and consequent glomerular injury. Furthermore, local inhibition of *Asc* gene completely abolished HFD-induced NALP3 inflammasome formation and activation, podocyte dysfunction and glomerular injury. Our results for the first time suggest that NALP3 inflammasome formation and activation are an important early mechanism responsible for glomerular inflammation and injury in obese mice.

We first characterized the Asc expression in renal tissue of $Asc^{-/-}$ and $Asc^{+/+}$ mice. We found that Asc expression was abolished in the kidneys of $Asc^{-/-}$ mice. These results suggest that the Asc gene is expressed in renal tissue and gene deletion in $Asc^{-/-}$ mice is successful. This suggests that the $Asc^{-/-}$ mice may be used for studies on the inflammatory mechanisms of obesity and obesity-associated organ damage. In this regard, it has been reported that inflammasomes associated with ASC, in particular, NALP3 inflammasome sense obesity-associated

danger signals and contribute to obesity-induced inflammation and insulin resistance [21,41]. Knockout of Nalp3 inflammasome significantly protects a mice model of HFD-induced obesity, insulin resistance, glucose intolerance and inflammation [21,41,51]. Moreover, the expression of NALP3 subunits in adipose tissue correlates directly with body weight in mouse models and obese individuals. Indeed, our results also showed that mice lacking *Asc* gene significantly attenuated the HFD-induced obesity compared to $Asc^{+/+}$ mice, indicating the role of NALP3 inflammasomes in obesity.

Recent studies demonstrated the role of NALP3 inflammasomes in chronic kidney diseases including hyperhomocysteinemia-induced glomerular injury, acute ischemia reperfusion-induced injury, unilateral ureteral obstruction and renal biopsies from patients with non-diabetic kidney diseases [25,26,37–40]. In the present study, we hypothesized that obesity activates the NALP3 inflammasome formation and activation in podocytes and thereby induce local sterile inflammation and glomerular injury. We demonstrated that HFD enhanced the inflammasome formation and increased production of IL-1β resulting in activation of inflammatory response in podocytes of obese $Asc^{+/+}$ mice, but not in $Asc^{-/-}$ mice. These results suggest that obesity-induced NALP3 inflammasome formation and activation occur in glomeruli of mice. Although this type of inflammasome was first characterized in immune cells, recent studies have demonstrated that it can be detected in various non-immune cells including intrinsic glomerular cells [37,39,52,53] and other residential cells in the brain, heart and vessels [54,55]. To our knowledge, these results represent the first experimental evidence demonstrating that obesity activates NALP3 inflammasomes in glomeruli of mice, which is an important pathogenic mechanism responsible for glomerular injury during obesity.

Using podocin as a podocyte marker, our confocal microscopic observations demonstrated that HFD-induced inflammasome formation in glomeruli was mostly located in podocytes, as demonstrated by the colocalization of Nalp3 with podocin. This colocalization was substantially blocked in mice lacking *Asc* gene. Another interesting finding of

Table 3
Asc mRNA expression in ND fed C57BL/6J WT mice with or without Asc shRNA transfection.

Parameters	Ctrl	Asc shRNA
Liver	1.0 ± 0.2	0.9 ± 0.2
Heart	1.0 ± 0.3	1.1 ± 0.2
Adipose tissue	1.0 ± 0.3	1.0 ± 0.1

Quantitative real time PCR analysis was performed and the values were normalized against β-actin. The data was expressed as mean ± SEM. N = 3–4 in each group. ND: Normal diet, Ctrl: Control (scramble shRNA).
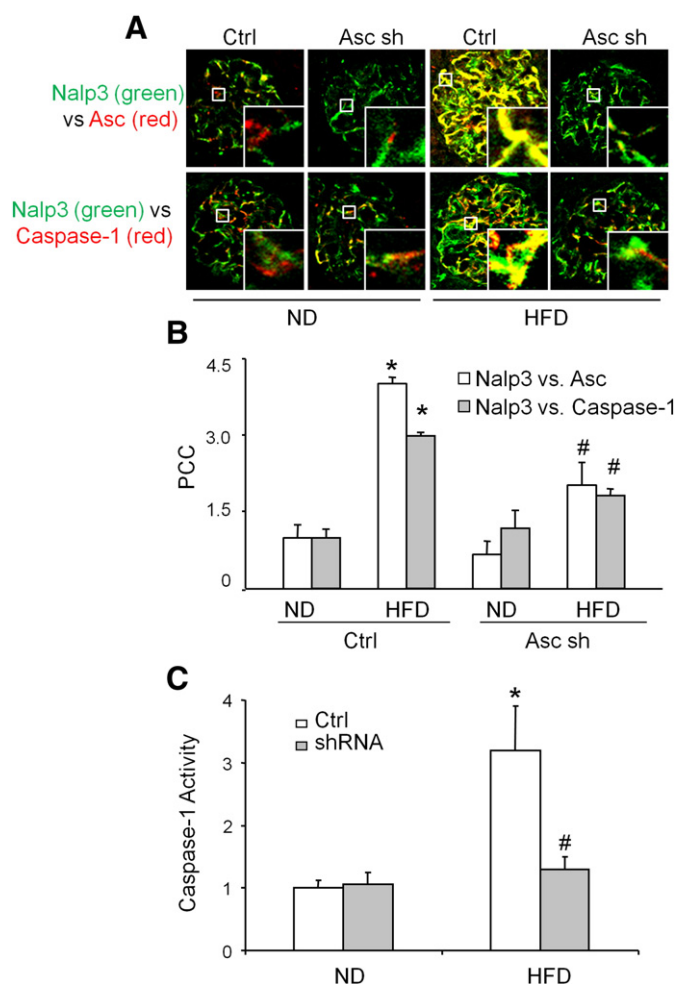
Fig. 7. Effects of renal Asc silencing on inflammasome formation and activation in C57BL/6J mice fed with ND or high fat diet. A. Overlaid images (yellow spots) show the colocalization of Nalp3 (green) with Asc (red) and Nalp3 (green) with caspase-1 (red) in mouse glomeruli. B. Values are arithmetic means ± SD (n = 6–8 each group) of caspase-1 activity in glomeruli of ND or HFD fed C57BL/6J WT mice with or without Asc shRNA transfection. *Significant difference ($P < 0.05$) compared to the values from control mice on the normal diet, #Significant difference ($P < 0.05$) compared to versus values from mice fed the HFD.

present study is that obesity directly induces podocyte dysfunction and injury in HFD-fed mice, as shown by decrease in podocin mRNA expression, increase in desmin expression, and foot process effacement. This HFD-induced podocyte injury was attenuated in mice lacking *Asc* gene. These results imply that podocytes are not only a glomerular cell type with intracellular inflammatory machinery featured by the formation and activation of inflammasomes, but also a cell type as a target of inflammatory factors derived from activated NALP3 inflammasomes. The present study did not aim to elucidate the exact mechanism mediating the effect of NALP3 inflammasome activation to directly induce podocyte injury. However, it may be due to the production of inflammatory factors such as IL-1β from activation of NALP3 inflammasomes, which may act in an autocrine or paracrine fashion to change podocyte function. Indeed, there were reports that various inflammatory factors including IL-1β can induce podocyte injury by reduction of nephrin production [52,56]. In addition, the non-inflammatory effects of NALP3 inflammasome activation such as pyroptosis, cytoskeleton changes and alteration of cell metabolism have also been reported to mediate the detrimental action of inflammasome activation [57–59].

Furthermore, we demonstrated that inhibition of inflammasome activation has a protective action on the glomerular injury associated with obesity. In accordance with decreased inflammasome formation

in $Asc^{-/-}$ mice on the HFD, urinary albumin excretion and glomerular injury and sclerosis were also significantly blocked compared with $Asc^{+/+}$ mice on the HFD suggesting that that inflammasome formation and activation are an important early mechanism responsible for glomerular inflammation and injury in obese mice. In particular, activation of podocyte or glomerular inflammasomes is critical for the development of glomerular injury associated with obesity. Therefore, the podocyte inflammasome associated with ASC as an intracellular inflammatory machinery or responder to endogenous danger factors could be a target of therapeutic strategy for obesity-induced glomerular injury or sclerosis.

To further address the role of key inflammasome adaptor protein *Asc* gene in mediating HFD-induced inflammasome formation and glomerular injury, a local gene silencing strategy was used in the present study, where an ultrasound microbubble-mediated plasmid delivery was employed to introduce Asc shRNA into the kidney. It was demonstrated that this method was highly efficient in delivering plasmids into renal cells in vivo. By an in vivo molecular imaging system to daily monitor the efficiency of Asc gene transfection in the kidney in living animals, we showed that the transgene or shRNA expression vector (with luciferase gene as an indicator) could be detected even 4 days after gene transfection and lasted for 4 weeks observed. This in vivo transgene monitoring importantly guided our functional studies to define the role of *Asc* gene in mediating inflammasome activation and glomerular damage associated with obesity. In such local *Asc* gene silenced kidney, we found that mRNA expression of Asc, colocalization of Nalp3 with Asc or caspase-1 in mouse glomeruli, caspase 1 activity and cleaved IL-1β production was significantly decreased. It was also demonstrated that silencing the *Asc* gene in the kidney ameliorates proteinuria and podocyte injury. These results from mice with local renal *Asc* gene silencing further support the conclusion above drawn from studies using $Asc^{-/-}$ mice that *Asc* inhibition or gene silencing abolishes HFD-induced action of inflammasome and thereby protect the kidney from obesity-associated glomerular injury. This protective action was observed not only in global deletion of *Asc* gene but also in locally silencing of this gene in glomeruli, further indicating that glomerular inflammasome may be a therapeutic target for prevention or treatment of obesity-induced glomerular sclerosis. This local gene silencing will exclude the possible effect of extra-renal gene deletion or silencing. However, the results from the present study remain to be elucidated in podocyte specific ASC inflammasome knockout mice. In conclusion, the present study demonstrated that inhibition of inflammasome activation by global *Asc* gene deletion or local *Asc* gene silencing attenuated the obesity-induced glomerular inflammation and injury. The amelioration of glomerular injury by Asc deficiency during obesity implicates the pivotal role of NALP3 inflammasomes in obesity-induced glomerulosclerosis. Targeting ASC-associated inflammasomes may be a novel therapeutic strategy for treatment and management of obesity and associated glomerular injury.

Acknowledgements

Appendix A. Supplementary data

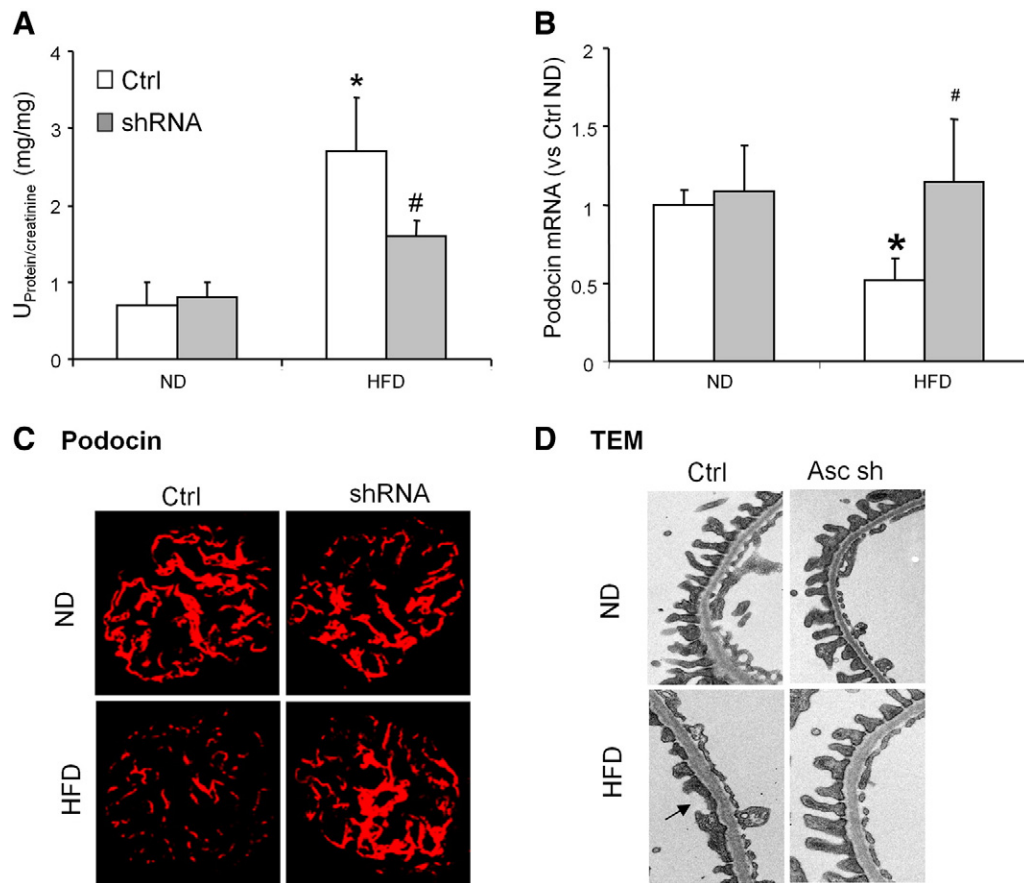Supplementary data to this article can be found online at http://dx.doi.org/10.1016/j.bbamcr.2014.01.033.

Fig. 8. Effects of renal Asc silencing on podocyte injury and glomerular injury in C57BL/6J mice fed with ND or high fat diet. A. Values are arithmetic means ± SD (n = 6–8 each group) of urinary protein excretion in C57BL/6J WT mice fed a ND or HFD with or without Asc shRNA transfection. B. Real-time RT-PCR analysis showing changes in the expression of podocin in glomeruli from different groups of mice (n = 6 per group). C. Typical images of podocin staining in glomeruli of C57BL/6J WT mice fed a ND or HFD with or without Asc shRNA transfection. D. *Asc* shRNA-improved podocyte ultrastructure in HFD treated mice as shown by TEM examinations. The arrow denotes the area of foot process effacement in $Asc^{+/+}$ mice on the HFD. Images are representative of 5 TEM images per kidney from 2 mice per group. *Significant difference ($P < 0.05$) compared to the values from control mice on the normal diet, #significant difference ($P < 0.05$) compared to versus values from mice fed the HFD.

References

[1] A.A. Hedley, C.L. Ogden, C.L. Johnson, M.D. Carroll, L.R. Curtin, K.M. Flegal, Prevalence of overweight and obesity among US children, adolescents, and adults, 1999–2002, JAMA 291 (2004) 2847–2850.

[2] S.F. Knight, J.D. Imig, Obesity, insulin resistance, and renal function, Microcirculation 14 (2007) 349–362.

[3] L.J. Ma, B.A. Corsa, J. Zhou, H. Yang, H. Li, Y.W. Tang, V.R. Babaev, A.S. Major, M.F. Linton, S. Fazio, T.E. Hunley, V. Kon, A.B. Fogo, Angiotensin type 1 receptor modulates macrophage polarization and renal injury in obesity, Am. J. Physiol. Renal Physiol. 300 (2011) F1203–F1213.

[4] C.L. Ogden, M.D. Carroll, L.R. Curtin, M.A. McDowell, C.J. Tabak, K.M. Flegal, Prevalence of overweight and obesity in the United States, 1999–2004, JAMA 295 (2006) 1549–1555.

[5] V. Thakur, S. Morse, E. Reisin, Functional and structural renal changes in the early stages of obesity, Contrib. Nephrol. 151 (2006) 135–150.

[6] S. Kassab, J. Novak, T. Miller, K. Kirchner, J. Granger, Role of endothelin in mediating the attenuated renal hemodynamics in Dahl salt-sensitive hypertension, Hypertension 30 (1997) 682–686.

[7] J.E. Hall, J.R. Henegar, T.M. Dwyer, J. Liu, A.A. Da Silva, J.J. Kuo, L. Tallam, Is obesity a major cause of chronic kidney disease? Adv. Ren. Replace. Ther. 11 (2004) 41–54.

[8] K.M. Boini, C. Zhang, M. Xia, W.Q. Han, C. Brimson, J.L. Poklis, P.L. Li, Visfatin-induced lipid raft redox signaling platforms and dysfunction in glomerular endothelial cells, Biochim. Biophys. Acta 1801 (2010) 1294–1304.

[9] J. Axelsson, O. Heimburger, P. Stenvinkel, Adipose tissue and inflammation in chronic kidney disease, Contrib. Nephrol. 151 (2006) 165–174.

[10] T.E. Hunley, L.J. Ma, V. Kon, Scope and mechanisms of obesity-related renal disease, Curr. Opin. Nephrol. Hypertens. 19 (2010) 227–234.

[11] S. Mariathasan, K. Newton, D.M. Monack, D. Vucic, D.M. French, W.P. Lee, M. Roose-Girma, S. Erickson, V.M. Dixit, Differential activation of the inflammasome by caspase-1 adaptors ASC and Ipaf, Nature 430 (2004) 213–218.

[12] S.L. Masters, E. Latz, L.A. O'Neill, The inflammasome in atherosclerosis and type 2 diabetes, Sci. Transl. Med. 3 (2011) 81 (ps17).

[13] P. Duewell, H. Kono, K.J. Rayner, C.M. Sirois, G. Vladimer, F.G. Bauernfeind, G.S. Abela, L. Franchi, G. Nunez, M. Schnurr, T. Espevik, E. Lien, K.A. Fitzgerald, K.L. Rock, K.J.

[14] A. Salminen, J. Ojala, T. Suuronen, K. Kaarniranta, A. Kauppinen, Amyloid-beta oligomers set fire to inflammasomes and induce Alzheimer's pathology, J. Cell. Mol. Med. 12 (2008) 2255–2262.

Moore, S.D. Wright, V. Hornung, E. Latz, NLRP3 inflammasomes are required for atherogenesis and activated by cholesterol crystals, Nature 464 (2010) 1357–1361.

[15] M.T. Heneka, M.P. Kummer, A. Stutz, A. Delekate, S. Schwartz, A. Vieira-Saecker, A. Griep, D. Axt, A. Remus, T.C. Tzeng, E. Gelpi, A. Halle, M. Korte, E. Latz, D.T. Golenbock, NLRP3 is activated in Alzheimer's disease and contributes to pathology in APP/PS1 mice, Nature 493 (2013) 674–678.

[16] D. De Nardo, E. Latz, NLRP3 inflammasomes link inflammation and metabolic disease, Trends Immunol. 32 (2011) 373–379.

[17] C. Dostert, V. Petrilli, R. Van Bruggen, C. Steele, B.T. Mossman, J. Tschopp, Innate immune activation through Nalp3 inflammasome sensing of asbestos and silica, Science 320 (2008) 674–677.

[18] T. Horng, G.S. Hotamisligil, Linking the inflammasome to obesity-related disease, Nat. Med. 17 (2011) 164–165.

[19] A.B. Imaeda, A. Watanabe, M.A. Sohail, S. Mahmood, M. Mohamadnejad, F.S. Sutterwala, R.A. Flavell, W.Z. Mehal, Acetaminophen-induced hepatotoxicity in mice is dependent on Tlr9 and the Nalp3 inflammasome, J. Clin. Invest. 119 (2009) 305–314.

[20] F. Martinon, V. Petrilli, A. Mayor, A. Tardivel, J. Tschopp, Gout-associated uric acid crystals activate the NALP3 inflammasome, Nature 440 (2006) 237–241.

[21] B. Vandanmagsar, Y.H. Youm, A. Ravussin, J.E. Galgani, K. Stadler, R.L. Mynatt, E. Ravussin, J.M. Stephens, V.D. Dixit, The NLRP3 inflammasome instigates obesity-induced inflammation and insulin resistance, Nat. Med. 17 (2011) 179–188.

[22] R. Zhou, A. Tardivel, B. Thorens, I. Choi, J. Tschopp, Thioredoxin-interacting protein links oxidative stress to inflammasome activation, Nat. Immunol. 11 (2010) 136–140.

[23] B.K. Davis, H. Wen, J.P. Ting, The inflammasome NLRs in immunity, inflammation, and associated diseases, Annu. Rev. Immunol. 29 (2011) 707–735.

[24] C. Faul, K. Asanuma, E. Yanagida-Asanuma, K. Kim, P. Mundel, Actin up: regulation of podocyte structure and function by components of the actin cytoskeleton, Trends Cell Biol. 17 (2007) 428–437.

[25] S.S. Iyer, W.P. Pulskens, J.J. Sadler, L.M. Butter, G.J. Teske, T.K. Ulland, S.C. Eisenbarth, S. Florquin, R.A. Flavell, J.C. Leemans, F.S. Sutterwala, Necrotic cells trigger a sterile

inflammatory response through the Nlrp3 inflammasome, Proc. Natl. Acad. Sci. U. S. A. 106 (2009) 20388–20393.

[26] C. Zhang, K.M. Boini, M. Xia, J.M. Abais, X. Li, Q. Liu, P.L. Li, Activation of Nod-like receptor protein 3 inflammasomes turns on podocyte injury and glomerular sclerosis in hyperhomocysteinemia, Hypertension 60 (2012) 154–162.

[27] Z.I. Niemir, H. Stein, G. Dworacki, P. Mundel, N. Koehl, B. Koch, F. Autschbach, K. Andrassy, E. Ritz, R. Waldherr, H.F. Otto, Podocytes are the major source of IL-1 alpha and IL-1 beta in human glomerulonephritides, Kidney Int. 52 (1997) 393–403.

[28] G.H. Tesch, N. Yang, H. Yu, H.Y. Lan, R. Foti, S.J. Chadban, R.C. Atkins, D.J. Nikolic-Paterson, Intrinsic renal cells are the major source of interleukin-1 beta synthesis in normal and diseased rat kidney, Nephrol. Dial. Transplant. 12 (1997) 1109–1115.

[29] G.L. Horvath, J.E. Schrum, C.M. De Nardo, E. Latz, Intracellular sensing of microbes and danger signals by the inflammasomes, Immunol. Rev. 243 (2011) 119–135.

[30] C. Jin, R.A. Flavell, Molecular mechanism of NLRP3 inflammasome activation, J. Clin. Immunol. 30 (2010) 628–631.

[31] M. Lamkanfi, V.M. Dixit, The inflammasomes, PLoS Pathog. 5 (2009) e1000510.

[32] M. Lamkanfi, L.V. Walle, T.D. Kanneganti, Deregulated inflammasome signaling in disease, Immunol. Rev. 243 (2011) 163–173.

[33] K. Schroder, J. Tschopp, The inflammasomes, Cell 140 (2010) 821–832.

[34] P.J. Shaw, M.F. McDermott, T.D. Kanneganti, Inflammasomes and autoimmunity, Trends Mol. Med. 17 (2011) 57–64.

[35] S.P. Wilson, S.L. Cassel, Inflammasome-mediated autoinflammatory disorders, Postgrad. Med. 122 (2010) 125–133.

[36] A. Halle, V. Hornung, G.C. Petzold, C.R. Stewart, B.G. Monks, T. Reinheckel, K.A. Fitzgerald, E. Latz, K.J. Moore, D.T. Golenbock, The NALP3 inflammasome is involved in the innate immune response to amyloid-beta, Nat. Immunol. 9 (2008) 857–865.

[37] H.J. Anders, D.A. Muruve, The inflammasomes in kidney disease, J. Am. Soc. Nephrol. 22 (2011) 1007–1018.

[38] A. Vilaysane, J. Chun, M.E. Seamone, W. Wang, R. Chin, S. Hirota, Y. Li, S.A. Clark, J. Tschopp, K. Trpkov, B.R. Hemmelgarn, P.L. Beck, D.A. Muruve, The NLRP3 inflammasome promotes renal inflammation and contributes to CKD, J. Am. Soc. Nephrol. 21 (2010) 1732–1744.

[39] A.A. Shigeoka, J.L. Mueller, A. Kambo, J.C. Mathison, A.J. King, W.F. Hall, J. da Silva Correia, R.J. Ulevitch, H.M. Hoffman, D.B. McKay, An inflammasome-independent role for epithelial-expressed Nlrp3 in renal ischemia–reperfusion injury, J. Immunol. 185 (2010) 6277–6285.

[40] C. Wang, Y. Pan, Q.Y. Zhang, F.M. Wang, L.D. Kong, Quercetin and allopurinol ameliorate kidney injury in STZ-treated rats with regulation of renal NLRP3 inflammasome activation and lipid accumulation, PLoS One 7 (2012) e38285.

[41] R. Stienstra, J.A. van Diepen, C.J. Tack, M.H. Zaki, F.L. van de Veerdonk, D. Perera, G.A. Neale, G.J. Hooiveld, A. Hijmans, I. Vroegrijk, S. van den Berg, J. Romijn, P.C. Rensen, L.A. Joosten, M.G. Netea, T.D. Kanneganti, Inflammasome is a central player in the induction of obesity and insulin resistance, Proc. Natl. Acad. Sci. U. S. A. 108 (2011) 15324–15329.

[42] N. Deji, S. Kume, S. Araki, M. Soumura, T. Sugimoto, K. Isshiki, M. Chin-Kanasaki, M. Sakaguchi, D. Koya, M. Haneda, A. Kashiwagi, T. Uzu, Structural and functional changes in the kidneys of high-fat diet-induced obese mice, Am. J. Physiol. Renal Physiol. 296 (2009) F118–F126.

[43] T. Jiang, Z. Wang, G. Proctor, S. Moskowitz, S.E. Liebman, T. Rogers, M.S. Lucia, J. Li, M. Levi, Diet-induced obesity in C57BL/6 J mice causes increased renal lipid accumulation and glomerulosclerosis via a sterol regulatory element-binding protein-1c-dependent pathway, J. Biol. Chem. 280 (2005) 32317–32325.

[44] A.E. Decleves, A.V. Mathew, R. Cunard, K. Sharma, AMPK mediates the initiation of kidney disease induced by a high-fat diet, J. Am. Soc. Nephrol. 22 (2011) 1846–1855.

[45] K.M. Boini, M. Xia, C. Li, C. Zhang, L.P. Payne, J.M. Abais, J.L. Poklis, P.B. Hylemon, P.L. Li, Acid sphingomyelinase gene deficiency ameliorates the hyperhomocysteinemia-induced glomerular injury in mice, Am. J. Pathol. 179 (2011) 2210–2219.

[46] J.M. Abais, C. Zhang, M. Xia, Q. Liu, T. Gehr, K.M. Boini, P.L. Li, NADPH oxidase-mediated triggering of inflammasome activation in mouse podocytes and glomeruli during hyperhomocysteinemia, Antioxid. Redox Signal. 18 (2013) 1537–1548.

[47] K.M. Boini, M. Xia, J. Xiong, C. Li, L.P. Payne, P.L. Li, Implication of CD38 gene in podocyte epithelial-to-mesenchymal transition and glomerular sclerosis, J. Cell. Mol. Med. 16 (2012) 1674–1685.

[48] K.M. Boini, C. Zhang, M. Xia, J.L. Poklis, P.L. Li, Role of sphingolipid mediator ceramide in obesity and renal injury in mice fed a high-fat diet, J. Pharmacol. Exp. Ther. 334 (2010) 839–846.

[49] C. Zhang, M. Xia, K.M. Boini, C.X. Li, J.M. Abais, X.X. Li, L.A. Laperle, P.L. Li, Epithelial-to-mesenchymal transition in podocytes mediated by activation of NADPH oxidase in hyperhomocysteinemia, Pflugers Arch. 462 (2011) 455–467.

[50] C. De Miguel, H. Lund, D.L. Mattson, High dietary protein exacerbates hypertension and renal damage in Dahl SS rats by increasing infiltrating immune cells in the kidney, Hypertension 57 (2011) 269–274.

[51] R. Stienstra, L.A. Joosten, T. Koenen, B. van Tits, J.A. van Diepen, S.A. van den Berg, P.C. Rensen, P.J. Voshol, G. Fantuzzi, A. Hijmans, S. Kersten, M. Muller, W.B. van den Berg, N. van Rooijen, M. Wabitsch, B.J. Kullberg, J.W. van der Meer, T. Kanneganti, C.J. Tack, M.G. Netea, The inflammasome-mediated caspase-1 activation controls adipocyte differentiation and insulin sensitivity, Cell Metab. 12 (2010) 593–605.

[52] J.R. Timoshanko, A.R. Kitching, Y. Iwakura, S.R. Holdsworth, P.G. Tipping, Leukocyte-derived interleukin-1beta interacts with renal interleukin-1 receptor I to promote renal tumor necrosis factor and glomerular injury in murine crescentic glomerulonephritis, Am. J. Pathol. 164 (2004) 1967–1977.

[53] J.R. Timoshanko, A.R. Kitching, Y. Iwakura, S.R. Holdsworth, P.G. Tipping, Contributions of IL-1beta and IL-1alpha to crescentic glomerulonephritis in mice, J. Am. Soc. Nephrol. 15 (2004) 910–918.

[54] W.R. Silverman, J.P. de Rivero Vaccari, S. Locovei, F. Qiu, S.K. Carlsson, E. Scemes, R.W. Keane, G. Dahl, The pannexin 1 channel activates the inflammasome in neurons and astrocytes, J. Biol. Chem. 284 (2009) 18143–18151.

[55] K. Yamasaki, J. Muto, K.R. Taylor, A.L. Cogen, D. Audish, J. Bertin, E.P. Grant, A.J. Coyle, A. Misaghi, H.M. Hoffman, R.L. Gallo, NLRP3/cryopyrin is necessary for interleukin-1beta (IL-1beta) release in response to hyaluronan, an endogenous trigger of inflammation in response to injury, J. Biol. Chem. 284 (2009) 12762–12771.

[56] Y. Takano, K. Yamauchi, K. Hayakawa, N. Hiramatsu, A. Kasai, M. Okamura, M. Yokouchi, A. Shitamura, J. Yao, M. Kitamura, Transcriptional suppression of nephrin in podocytes by macrophages: roles of inflammatory cytokines and involvement of the PI3K/Akt pathway, FEBS Lett. 581 (2007) 421–426.

[57] G.Y. Chen, G. Nunez, Sterile inflammation: sensing and reacting to damage, Nat. Rev. Immunol. 10 (2010) 826–837.

[58] M. Lamkanfi, Emerging inflammasome effector mechanisms, Nat. Rev. Immunol. 11 (2011) 213–220.

[59] F. Martinon, K. Burns, J. Tschopp, The inflammasome: a molecular platform triggering activation of inflammatory caspases and processing of proIL-beta, Mol. Cell 10 (2002) 417–426.